AMS 8th Conference on Aviation Range and Aerospace Meteorology
10-15 January 1999, Dallas, Texas

9.5 GMS-5 AND NOAA AVHRR SATELLITE OBSERVATIONS OF THE NEW ZEALAND MT RUAPEHU ERUPTION OF 19/20 JULY 1996

Rodney Potts[1] and Masami Tokuno[2]
1. Bureau of Meteorology Research Centre, Australia
2. Meteorological Satellite Center, JMA, Japan

1. INTRODUCTION

Research has shown that satellite data can be used to detect volcanic ash clouds and monitor their movement and these data are important for operational staff responsible for providing warnings for volcanic ash for aviation. There are a number of limitations in the utility of currently available satellite data for identifying volcanic ash clouds, particularly in discriminating the ash from water/ice clouds. Further research has therefore been directed to better use of currently available data for identifying volcanic ash clouds and investigating the utility of additional satellite data which will become available in the future with the launch of more advanced satellites.

Studies have shown the difference in brightness temperature between the water vapour window channels in USA National Oceanographic and Atmospheric Administration (NOAA) advanced very high resolution radiometer (AVHRR) imagery (10.8 and 12.0 microns) can improve the discrimination of ash from water/ice clouds (Prata, 1989; Potts, 1993; Tokuno, 1997). This results from the difference in wavelength dependence of emissivity for water/ice and the silicates in ash. The temperature difference is often small and in using these data the observed radiances must be determined accurately with consideration given to calibration (Potts and Ebert, 1996) and registration of the sensor data in the different bands. Also, the characteristic difference indicating the presence of ash may not be evident where there is a high concentration of water or ice (Rose et al., 1995) and "false detections" may occur in areas of deep convection which penetrate the tropopause (Potts and Ebert, 1996). Nevertheless, these data are of operational value for detecting volcanic ash and monitoring its movement when used with standard visible and infrared imagery.

At middle and low latitudes with two polar orbiting NOAA satellites, for example NOAA 12 and 14, the AVHRR data are available at intervals of 3 - 6 hours which is less frequent than operationally desirable. In 1995 the Japanese geostationary satellite GMS-5 became operational providing data at hourly intervals over the volcanically active Asia/Pacific region. Besides visible and water vapour channels this satellite provides data in two infrared channels similar to the AVHRR, offering the potential for more timely detection of volcanic ash over the region.

On 19 July 1996, Mt Ruapehu (39°17′ S, 175°34′E, elevation 2796 m), one of New Zealands most active volcanoes erupted causing considerable disruption to aviation operations over much of the North Island of New Zealand. In this paper we examine GMS-5 and NOAA AVHRR satellite data for this eruption and compare the utility of these data for discriminating volcanic ash from water/ice clouds.

2. SATELLITE CHARACTERISTICS

Sensor characteristics for the NOAA-12 and NOAA-14 AVHRR and those on GMS-5, located over the equator at longitude 140 deg E, are shown in Table 1. This shows the GMS-5 infrared data has a reduced spatial resolution and a reduced temperature resolution due to the lower level of digitisation. The response characteristics for the GMS5 IR1 and IR2 sensors also have an increased overlap in comparison to the NOAA AVHRR Channel 4 and 5 sensors (The GMS Users Guide 1997).

	NOAA 12 / 14	GMS-5
Sensors (μm)	Ch 1: 0.58 - 0.68	VIS: 0.55 - 0.9
	Ch 2: 0.725 - 1.1	
	Ch 3: 3.55 - 3.93	IR3: 6.5 - 7.0
	Ch 4: 10.3 - 11.3	IR1: 10.5 - 11.5
	Ch 5: 11.5 - 12.5	IR2: 11.5 - 12.5
Nadir res. (km)	1.1 (all channels)	VIS: 1.25
		IR: 5.0
NE**Δ**T	0.12 K at 300 K	≤0.355K at 300K (IR1, IR2) ≤0.22K at 300K (IR3)
		≤1.00K at 220K (IR1) ≤0.90K at 220K (IR2) ≤1.5K at 220K (IR3)
Digitisation	VIS: 1024 level	VIS: 64 level
	IR: 1024 level	IR: 256 level

Table 1. Sensor characteristics for GMS-5 and NOAA-12/14 satellites.

* *Corresponding author address*: Rodney Potts, Bureau of Meteorology Research Centre, 150 Lonsdale St, Melbourne, VIC 3000, AUSTRALIA. email: R.Potts@bom.gov.au

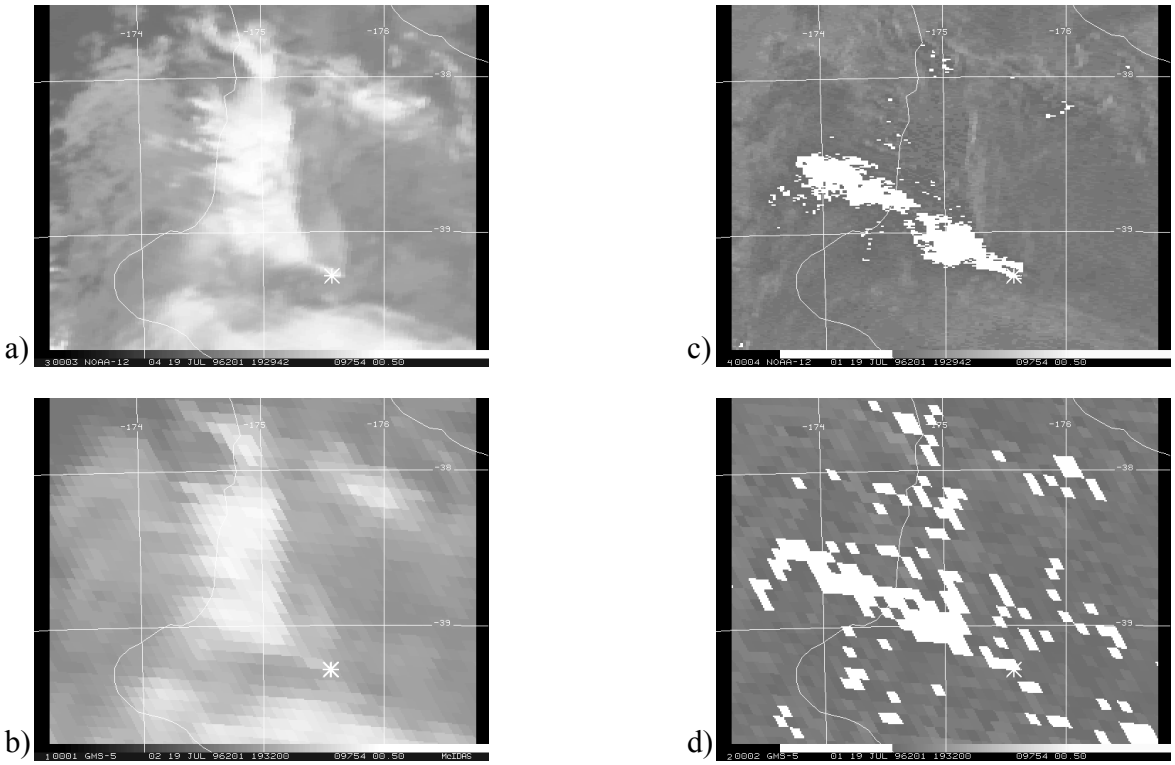

Figure 1. NOAA AVHRR images for 19 July 1996, 1934 UTC of (a) channel 4 brightness temperature (T4), and (c) temperature difference (T4-T5). GMS-5 images for 19 July 1996, 1951 UTC of (b) IR1 brightness temperature and (d) temperature difference (IR1-IR2). Images are in Lambert conformal projection and times correspond to the scan time at the latitude of the volcano which is indicated.

3. SATELLITE OBSERVATIONS OF RUAPEHU ERUPTION

Mt Ruapehu erupted at 1200 UTC on 19 July and the eruption continued for approximately 24 hours (Mann, 1998). Strong seismic activity occurred in the period 1200 - 1900 UTC, followed by a period of weak seismic activity and then a number of strong seismic events in the period 0100 - 0700 UTC, 20 July. In this study we concentrate on the initial period of strong volcanic activity only. Although there was cloud present in the area, the plume from the initial eruption was evident in both GMS-5 and NOAA AVHRR satellite imagery. The eruption plume was initially carried to the southwest and west but after several hours it moved to the north and then the northeast.

Figures 1(a) and 1(b) show the NOAA 12 AVHRR Channel 4 image for 1934 UTC and the GMS-5 IR1 image for 1951 UTC respectively with the eruption plume extending to the west and northwest of the volcano. To enable a direct comparison the satellite data has been remapped to a Lambert conformal projection after first correcting for errors in the navigation. The corresponding brightness temperature differences (T4-T5) and (IR1-IR2) were also calculated and are shown in Figures 1(c) and 1(d). In these figures the areas of negative differences are shown as white (indicating possible ash) while the areas of positive differences are shown as grey (indicative of clear sky and water/ice clouds).

Fig.1(c) shows the area of negative differences extends to the west of the apparent plume boundary in Fig.1(a) and indicates the presence of dispersed ash with little associated water or ice cloud. The positive differences in the northern parts of the apparent plume suggest that any ash particles are mixed or coated with water or ice.

In the analysis of the GMS-5 IR1-IR2 data, some mis-registration of the IR1 and IR2 data in the element direction was evident. This was corrected by a simple interpolation of the IR2 brightness temperature in the element direction by the equivalent of approximately +0.7 km and calculating the difference between IR1 and the interpolated IR2 temperatures. The remaining single-pixel ‘speckles’ in Fig. 1(d) where IR1-IR2 < 0 can be largely attributed to the effect of sub-pixel cloud elements and the non-uniform sensor response within the pixel area. This causes irregular temperature variations between adjacent pixels and introduces small errors when calculating the interpolated temperature.

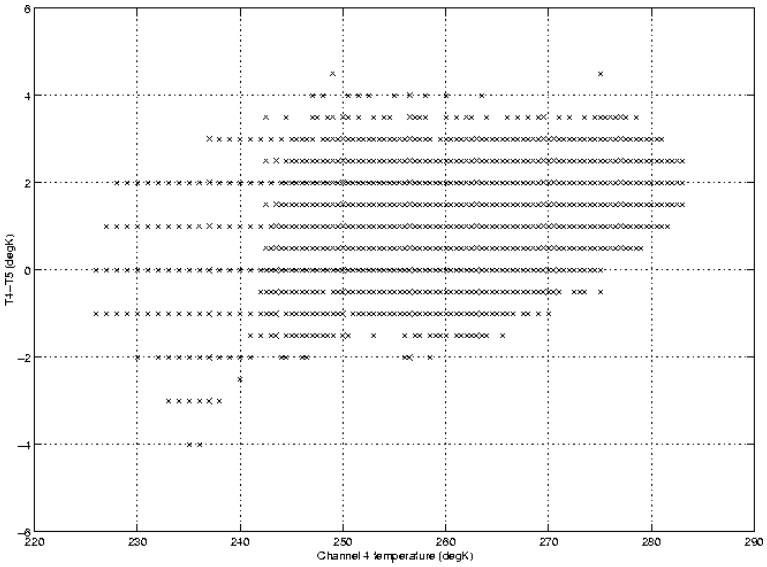

Figure 2a. Scatter diagram showing brightness temperature difference (T4-T5) as function of T4 for AVHRR image of Fig.1a.

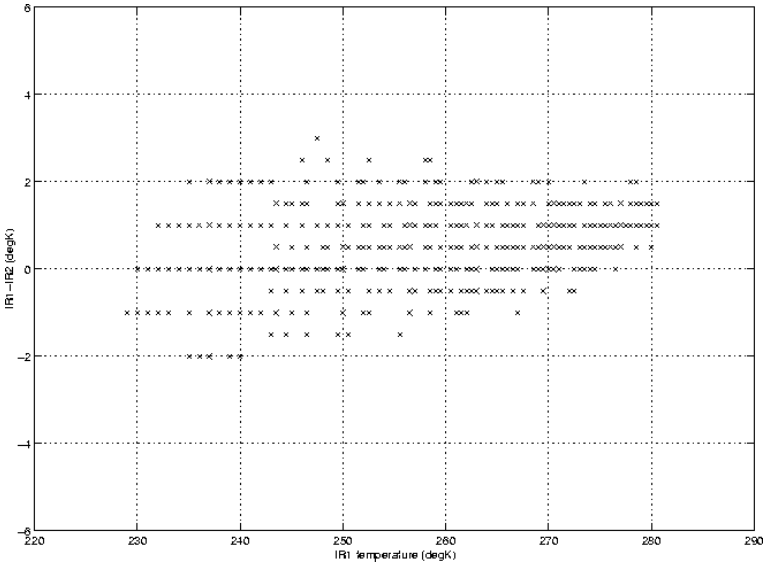

Figure 2b. Scatter diagram showing brightness temperature difference (IR1-IR2) as function of IR1 for GMS-5 image of Fig.1c.

Figure 1 shows good correspondence between the NOAA AVHRR T4-T5 data and the GMS-5 IR1-IR2 data given the differences in the spatial resolution, temperature resolution, sensor response characteristics and the observation time. Scatter plots of the AVHRR T4-T5 vs T4 data and GMS-5 IR1-IR2 vs IR1 data for the areas shown in Fig.1 were prepared (Fig.2) and also show good correspondence. The reduced differences in the GMS-5 data (Fig.2(b)) compared with AVHRR data (Fig.2(a)) are consistent with theoretical expectations given the reduced temperature resolution and greater overlap in the sensor response (Tokuno, 1997).

The GMS-5 data is available hourly and Figures 3(a) - 3(d) show 2-hourly GMS-5 IR1 images of the eruption plume for the period 1551 - 2151 UTC. These data have also been remapped to a Lambert conformal projection after first correcting for errors in the navigation. Images of the brightness temperature difference (IR1-IR2) for the same times are shown in Figures 3(e) - 3(h). The approximate boundary of the ash plume is shown, determined from a manual examination of the hourly infrared and IR1-IR2 imagery and a loop of these images.

Early in the period following the eruption the plume moved over a band of pre-existing cloud. The minimum observed brightness temperature for the plume in this period was 225 K, slightly colder than the surrounding cloud and indicating the plume extended above the cloud. Based on the vertical temperature and wind profiles for 1200 UTC, 19 July, and 0000 UTC, 20 July, from the meteorological office at Paraparaumu (40°33′ S, 170° E) and assuming black body radiation this corresponds to a height of 8.5 km.

By 2155 UTC the cloud and ash plume had thinned significantly, due to evaporation of the water/ice cloud and dispersion of the ash, and observed brightness temperatures increased due to increasing radiance from lower layers of the atmosphere.

Figures 3(e) - (h) show negative differences indicative of the presence of volcanic ash though it is not until 1951 UTC that a well defined and significant area is evident, some 7-hours after the eruption began. Before this time the negative differences typically associated with ash were not evident indicating a mix of ash and water/ice in the plume. The most-negative differences were observed at 2151 UTC when the cloud had largely dissipated and ash become more disperse. Following this the plume moved to the northeast and dispersed further. An area of negative differences associated with this plume was evident until 0251 UTC.

Figures 1 and 3 show the brightness temperature difference IR1-IR2 for the GMS-5 data display a characteristic difference for water/ice clouds and volcanic ash clouds similar to that evident in the NOAA AVHRR data. This characteristic difference is more well defined in the AVHRR data because of the improved spatial and temperature resolution and similar gains should be achieved in the future with the launch of more advanced geostationary satellites over the Asia/Pacific region.

Dependent on the magnitude of an eruption and the pattern of upper level winds an eruption plume can disperse rapidly and the hourly GMS-5 data enables more timely detection of the plume and the movement to be better monitored. In particular the ability to view hourly visible, infra red and IR1-IR2 imagery as a loop enables a better determination of the boundary of an ash plume and its movement. More accurate warnings can be provided and a more valid assessment of the accuracy of volcanic ash trajectory forecast models can be made.

Finally, we have seen that the characteristic difference indicating the presence of ash may not be evident in areas where there is a high concentration of water/ice in an eruption plume. This limits the operational effectiveness of these data and it is clear that further research is required to develop techniques which enable the more timely detection of volcanic ash.

4. CONCLUSIONS

In this study we examine GMS-5 and NOAA AVHRR satellite data for the 19 July 1996 eruption of the Ruapehu volcano in New Zealand to compare the utility of these data for the discrimination of volcanic ash from water/ice clouds. We show the brightness temperature difference (IR1-IR2) displays a characteristic difference for water/ice clouds and volcanic ash clouds similar to that evident in the NOAA AVHRR data though less well defined because of the reduced spatial and temperature resolution. The ability to view hourly visible, infra red and IR1-IR2 imagery as a loop is a valuable aid for the determination of the boundary of an ash plume and its movement. It is also clear there is a need to further improve the discrimination of water/ice clouds from volcanic ash clouds if more timely information is to be provided and appropriate research is required.

5. REFERENCES

Mann N.K., 1998: X-Band radar measurements of volcanic ash plumes: Ruapehu eruption 1996. MSc Thesis. University of Auckland.

Potts R.J., 1993: Satellite observations of Mt Pinatubo ash clouds. Aust. Met. Mag. 42, 59-68.

Potts R.J., and Ebert E., 1996: On the detection of volcanic ash in NOAA AVHRR infrared satellite imagery. Proceedings of the 8th Australasian Remote Sensing Conference, 25-26 March 1996, Canberra, Australia.

Prata A.J., 1989: Infrared radiative transfer calculations for volcanic ash clouds. Geophys. Res. Letters. 16, 1293-6.

Rose W.I., Delene D.J., Schneider D.J., Bluth G.J.S., Krueger A.J., Sprod I., McKee C., Davies H.L., and Ernst G.G.J., 1995: Ice in the 1994 Rabaul eruption cloud: Implications for volcano hazard and atmospheric effects. Nature, 375, 477-479.

The GMS Users Guide Third Edition 1997: Meteorological Satellite Center, Japan Meteorological Agency.

Tokuno M., 1997: Satellite observation of volcanic ash clouds. Meteorological Satellite Centre Technical Note No.33, pp 29-48. Japan Meteorological Agency.

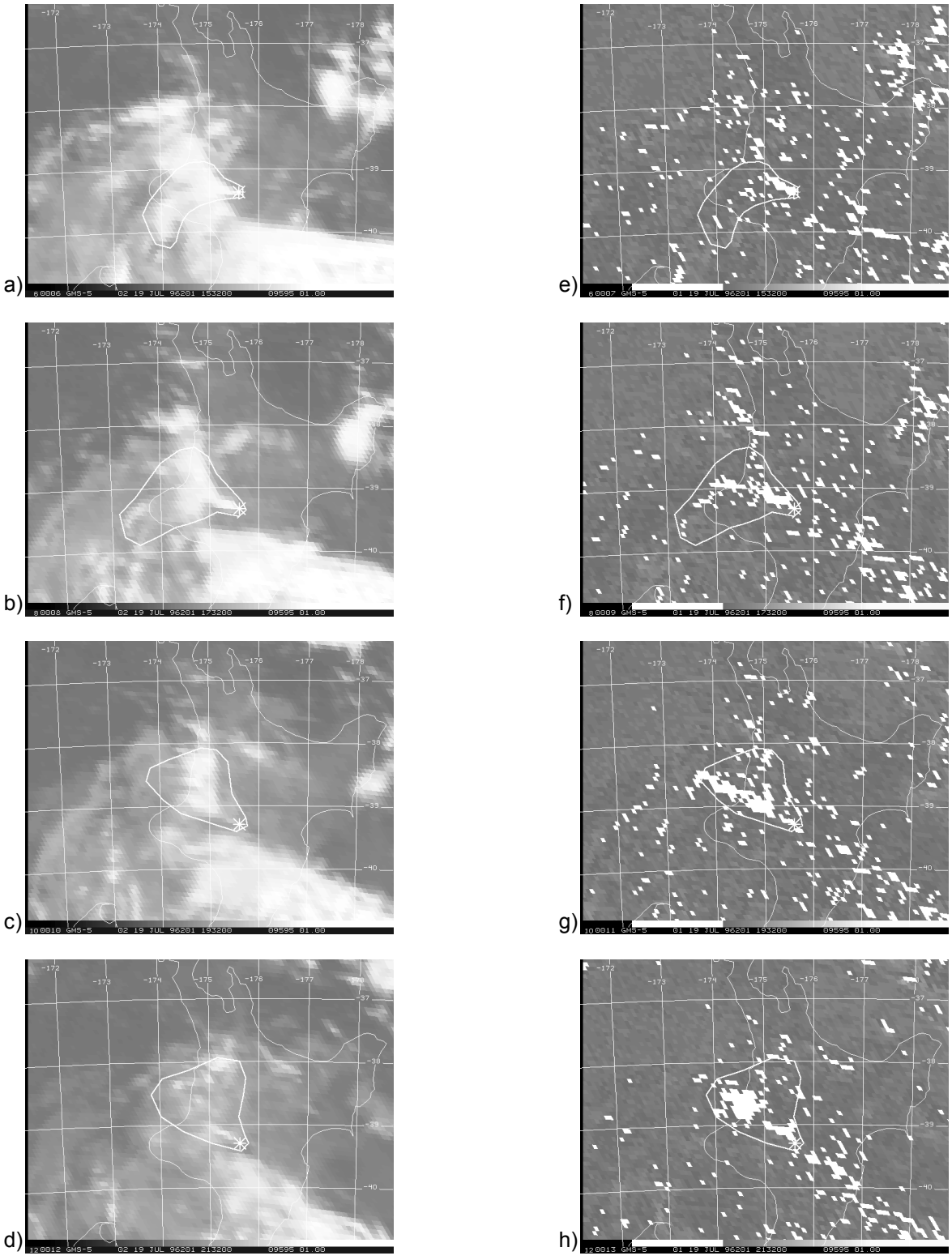

Figure 3. GMS-5 images of Ruapehu eruption of 19 July 1996. Shown are IR1 images of (a) 1551 UTC, (b) 1751 UTC, (c) 1951 UTC, and (d) 2155 UTC; and images of the temperature difference IR1-IR2 for the same times ((e)-(f)). Images are in Lambert conformal projection and times correspond to the scan time at the latitude of the volcano.